On the Evaluation of Biological Effects of Wearable Antennas on Contact with Dispersive Medium in Terms of SAR and Bio-Heat by Using FIT Technique

Tommi Tuovinen, Markus Berg, Kamya Yekeh Yazdandoost, Matti Hämäläinen, Jari Iinatti

Centre for Wireless Communications
University of Oulu
Oulu, Finland
{forename.surname}@ee.oulu.fi

***Abstract*—Considerations of biological effects, executed as the bio-heat and bio-thermal simulations, in terms of a specific absorption rate (*SAR*) and temperature rise in human body tissues for ultra wideband (UWB) wireless body area network (WBAN) applications are studied in this paper. 3D-electromagnetic (EM) simulation software, utilizing finite integration technique (FIT), is used in order to obtain temperatures and power losses by thermal stationary and transient solvers (TSS, TTS) in the vicinity of the modelled dispersive medium. Two different UWB antennas having excellent radiation properties are experimented on contact with tissues. The effect of the antenna input power on the temperature and maximum *SAR*s over 1 g and 10 g averaging masses are evaluated. Obtained results are compared with the restrictions set by the institute of Electrical and Electronics Engineers (IEEE) and International Commission on Non-Ionizing Radiation Protection (ICNIRP). This paper investigates generally how much power should be fed to the UWB antenna in order to cross the maximum *SAR* limits in WBANs or in order the antenna start to heat the tissues significantly, both in the stationary conditions and further as the transient solutions.**

Keywords—specific absorption rate (SAR); temperature rise in tissues; wireless body area network (WBAN)

I. INTRODUCTION

In wireless body area network (WBAN) applications, a measurement device targeted for recording the decided parameters includes both a sensor and an antenna. Therefore it might cause the certain exposure level of an electromagnetic (EM) radiation depending on the emitted power of the device [1]. Once the device is used on the body over a long period of time, the temperature rise should be limited and controlled in advance in order to avoid the heat generation and harmful effects on tissues. Actual exposure to EM fields is regulated according to standardization guidelines [2], [3]. Fundamentally, human body is formed of water, electrolytes, and molecules, which have certain dipolar momentum that is able to interact with the E-field [1]. It is explained in [1], if the E-field propagates through the tissues, EM energy turns into the heat due to the dielectric losses, which means that as long as the E-field travels across the body, its energy decrease resulting in the temperature increase around its surrounding tissues. Federal Communications Commission (FCC) recommends to investigate specific absorption rate (*SAR*) in order to evaluate the radio frequency (RF) exposure level [4]. Nowadays, the most commonly used *SAR* limits are defined both by the Institute of Electrical and Electronics Engineers (IEEE) [2] (1.6 mW/g) for any 1 g of tissue and the International Commission on Non-Ionizing Radiation Protection (ICNIRP) [3] (2 mW/g) for any 10 g of tissue. These guidelines are adjusted in terms of the maximum mass-normalised rates of EM energy deposition for any 1 g or 10 g of tissue [5]. However, some exceptions are also shown, e.g., that hands and feet are excluded where higher *SAR*s up to 4 mW/g (for 10 g) are permitted in both of these standards [5].

It is possible to realize thermal modelling by contemporary simulation software. From the perspective of modelling, it is both efficient and safe, because software enables to execute investigations without human subject under tests, and additionally, the optimal antenna positions from the bio-heat point of view can be relatively easily obtained. Only few investigations have been realized so far for examining some of biological effects, e.g., *SAR* especially for ultra wideband (UWB) WBAN applications [6], [7]. Therefore, for observing the foregoing biological effects, two different planar UWB antennas having excellent radiation properties are exploited for the bio-heat and bio-thermal simulations in this paper. The temperature rise and power losses with time in tissues are solved by using thermal stationary and transient solvers (TSS, TTS) with computer simulation technology (CST) microwave studio (MWS) suite software using finite integration technique (FIT) [8]. Antennas are positioned on contact with a layered tissue model, for which the frequency-dependent behaviour based on the Debye 2nd order model is defined. In this paper, we present an approach to investigate how much (input) power can be fed to the antenna from the *SAR* and temperature rise perspective in order the human body tissues are in safe. This paper not only considers and examines different input powers, but also the heat generation in different tissues is of interest as well.

This paper is structured as follows. Section II considers the heat generation in tissues and *SAR*, and also describes the simulation method, setup and antennas. In Section III, the results of this work are shown and explained by following conclusions and possible future work, provided in Section IV.

978-1-4673-5772-2/13/$31.00 ©2013 IEEE

TABLE I. REQUIRED BIO-THERMAL SIMULATION PROPERTIES FOR TISSUES, ANTENNA SUBSTRATE AND ANTENNA COPPERING

Thermal Properties	Human Body Tissues			TRF-43 Antenna Substrate	Antenna Coppering
	Skin	*Fat*	*Muscle*		
Thermal conductivity, K [W/K/m]	0.293	0.201	0.530	0.43	5.96×10^{-7}
Heat capacity, C [kJ/K/kg]	3.5	2.5	3.5	0.92	0.4
Thermal diffusivity, d [m^2/s] $\times 10^{-8}$	7.61	8.78	14.36	0.19×10^{-3}	0.12×10^{-3}
Density ρ [kg/m^3]	1100	916	1041	2.46	-

II. HEAT GENERATION AND SAR IN SIMULATIONS

A. Background Information

The heat generation in tissues due to EM waves is fundamentally discussed in [1], [9]. EM energy starts to heat the tissues after the E-field has been passed through and penetrating tissues. An original Bio-heat Equation can be used for the estimation of temperature increase within tissues as [1]

$$C\rho \frac{\partial T}{\partial t} = \mathrm{K} \cdot \nabla^2 T + h_m + h_b, \quad (1)$$

where C is the specific heat [kJ/K/kg], T the tissue temperature [K], K the thermal conductivity [W/K/m], h_m the rate of tissue heat production, and h_b the rate of heat transfer from blood tissue. As explained in [1], (1) simply equals to how much temperature increases per unit time when multiplied by the thermal capacitance of 1 m^3 of tissue, to the heat accumulated per unit time and per unit volume in the body. For calculating the temperature in tissues by simulations, the used parameters for tissues are presented in Table I.

SAR can be defined with the tissue conductivity σ [S/m] multiplied with the rms value of E-field $|\boldsymbol{E}|$ (or E-field strength E) further divided by the tissue density ρ [kg/m^3] [1]

$$SAR = \frac{\sigma}{\rho}|\boldsymbol{E}|^2 = \frac{\sigma E^2}{2\rho}. \quad (2)$$

CST C95.3 averaging method that corresponds to IEEE C95.3 is used [2]. The maximum values of mass-averaged *SAR*s over both 10 g and 1 g averaging mass are studied here.

B. Simulation Methods

Bio-thermal simulations are implemented by obtaining first the time domain transient (TDT) solution for the simulation model by using the Gaussian pulses as an excitation signal in CST MWS. In TDT runs, power losses are recorded with power loss monitors (PLMs) by following the conversion of RF losses into the temperature distributions, executed as the calculation of thermal loss distributions from TDT solution, which are further imported as an excitation source for the thermal solver in CST microphysics (MP). In CST MP, TTS and TSS are used to obtain the required thermal properties. For TTS, the smooth step signal with the signal rise time T_{RISE} of 10 s (arise: 80 %) and total signal time T_{TOTAL} of 720 s are exploited as an excitation. Practically, the preliminary temperatures in the stationary situation are first attained with the certain rms power scaling factors (*PSF*s) (which

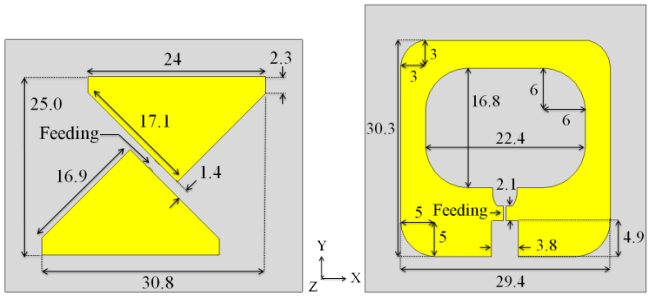

Figure 1. The CST simulation models of the planar UWB antennas (with TRF-43 antenna substrate) for the investigations: bow-tie dipole (left), and loop (right) antenna.

corresponds to peak input power (*PIP*) when multiplied by two) by using TSS. Next, in order to clarify a time-temperature dependency, simulations with TTS are run for obtaining a transient increase of the temperature of tissues over the period of 12 minutes (720 seconds). The IEEE C95.3 standard recommends recording temperature over the period of 6 minutes. Here, different *PSF*s for each simulation case discussed in the next Section are considered such that *PIP*s through 0.5 mW < *PIP* < 250 mW were used. In calculations, an initial temperature of 36 ºC is adjusted.

In *SAR* simulations, only TDT simulations for the adjusted PLMs are recorded, and different *SAR* results for the certain average cubes are calculated with the post-processing templates for different rms reference powers, i.e., again equal to *PIP* if multiplied by two.

C. Simulation Setup and Antennas

Four different tissue-equivalent slab models are studied for investigations. First model (i.e., later called as M1) is made of skin (thickness t = 2 mm), fat (t = 3 mm), and muscle (t = 30 mm) tissues with the total size of 300 mm (x) · 300 mm (y) · 35 mm (z). Three other tissue models are made only of skin (M2), fat (M3) or muscle (M4) also with the same total size of 300 mm (x) · 300 mm (y) · 35 mm (z), for demonstrating how the SAR and temperature results vary between these different configurations. The broadband behaviour for tissues is generated based on the 2nd order Debye dispersion model, which Equations and used values are described earlier, e.g., in [11], [12]. Two planar UWB antennas are used in the examinations, which are presented in Fig. 1: a) bow-tie dipole (presented already in [10], [11]), and b) single loop (not published earlier). For the same reasons (referring to some lacks with the practical on body usage of FR4) described in [12], an alternative substrate material, the 1.63 mm thick polytetrafluoroethylene-based (PTFE) TRF-43 [13], is also experimented for these antennas.

TABLE II. *SAR*S WITH DIFFERENT PEAK INPUT POWERS (*PIP*S) IN CASE THE ANTENNA CONTACTS THE TISSUE MODEL. NOTE DIFFERENT *PIP*S FOR 10 G AND 1 G CUBES. MODEL M1 INCLUDES SKIN (T = 2 MM), FAT (T = 3 MM), AND MUSCLE (T = 30 MM) TISSUES, M2 ONLY SKIN (T = 35 MM), M3 FAT, AND M4 MUSCLES

PIP [mW]	**Bow-Tie Dipole**				**Single Loop**				***PIP*** [mW]	**Bow-Tie Dipole**				**Single Loop**			
	10 g cube				***10 g cube***					***1 g cube***				***1 g cube***			
	Frequency [GHz]				***Frequency*** [GHz]					***Frequency*** [GHz]				***Frequency*** [GHz]			
	3	5	7	9	3	5	7	9		3	5	7	9	3	5	7	9
M1	ICNIRP SAR limit = 2.0 mW/g for 10 g cube								**M1**	IEEE SAR limit = 1.6 mW/g for 1 g cube							
0.5	0.01	0.01	0.01	0.01	0.01	0.01	0.01	0.01	0.5	0.03	0.04	0.04	0.03	0.04	0.06	0.05	0.05
25	0.56	0.65	0.62	0.55	0.50	0.64	0.58	0.47	15	0.92	1.22	1.14	0.91	1.17	1.60	1.42	1.46
100	2.23	2.60	2.48	2.21	2.01	2.56	2.30	1.90	25	1.53	2.03	1.91	1.52	1.95	2.67	2.36	2.43
M2									**M2**								
0.5	0.01	0.01	0.01	0.02	0.01	0.01	0.02	0.01	0.5	0.05	0.06	0.07	0.07	0.05	0.05	0.06	0.07
25	0.67	0.72	0.74	0.75	0.70	0.75	0.77	0.75	15	1.56	1.87	2.00	2.01	1.41	1.46	1.80	1.96
100	2.68	2.88	2.96	3.02	2.81	2.97	3.08	2.98	25	2.60	3.12	3.34	3.35	2.36	2.43	3.00	3.26
M3									**M3**								
0.5	0.00	0.00	0.00	0.00	0.00	0.00	0.00	0.00	0.5	0.00	0.00	0.01	0.00	0.00	0.00	0.01	0.01
25	0.08	0.09	0.11	0.09	0.09	0.10	0.12	0.11	15	0.08	0.13	0.17	0.12	0.13	0.15	0.18	0.15
100	0.30	0.35	0.44	0.37	0.36	0.40	0.47	0.43	25	0.13	0.22	0.29	0.20	0.21	0.25	0.30	0.26
M4									**M4**								
0.5	0.02	0.02	0.02	0.02	0.01	0.02	0.02	0.01	0.5	0.04	0.05	0.05	0.05	0.04	0.04	0.06	0.06
25	0.79	0.83	0.84	0.81	0.72	0.78	0.80	0.75	15	1.24	1.36	1.44	1.39	1.29	1.36	1.66	1.86
100	3.14	3.30	3.36	3.22	2.87	3.11	3.22	2.98	25	2.06	2.27	2.39	2.31	2.15	2.27	2.76	3.10

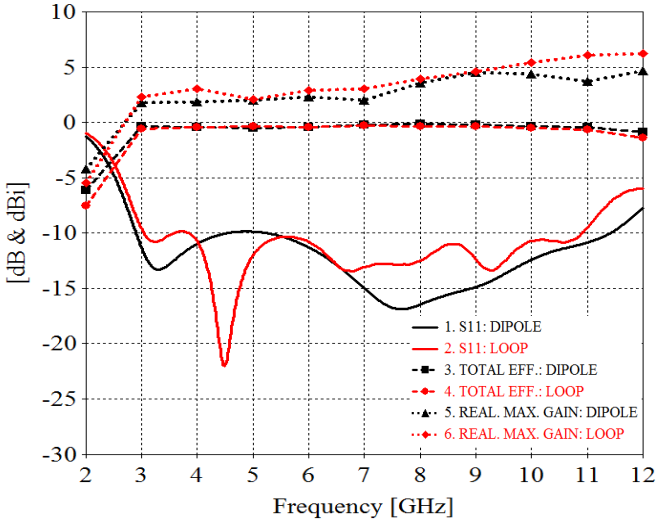

Figure 2. FS simulation results for investigated antennas: reflection coefficient S_{11} [dB], total antenna efficiency [dB], and realized maximum gain [dBi].

III. RESULTS

In the first phase, the free space (FS) performance between exploited antennas under investigations was compared and they were concluded to be very close to each other, as depicted in Fig. 2. As shown there, the reflection coefficient S_{11}, total antenna efficiency and realized maximum gain of these antennas are quite similar. Then, the effect of both different *PIP*s on the *SAR* results and stationary temperatures were evaluated by following the investigations of corresponding *PIP*s for time-dependent temperatures. Both the *SAR* and temperature results were examined on contact with different tissue models in order to receive some basic knowledge how different tissues in the outer layers of human body influence on the biological effects, and on the other hand, if there are any significant differences between them.

A. The Effect of Power Fed to the Antenna

1) SAR

The maximum *SAR*s over 1 g cube with different input powers collected to Table II were first investigated and compared with the IEEE *SAR* limit close to tissue models. We started the evaluations by using very low *PIP* of 0.5 mW and *SAR* values were observed to be far below the safety limits. As we have assumed the model M1 to be a good assumption for the tissue combination in the abdomen of human, the amount of *PIP* should be roughly as high as 25 mW in order to exceed the IEEE *SAR* limit. Then, the maximum *SAR*s over 10 g averaging mass were evaluated in the proximity of the same models. In these cases, achieved values are compared with the ICNIRP *SAR* limit. Like over the 1 g cube, also the results over the 10 g cube with *PIP* = 0.5 mW were observed to appear very small in proportion to the safety guidelines. For 10 g cube, the *PIP* of 100 mW was observed to be enough to cross the ICNIRP *SAR* limit. Further, the effect of different tissues on the *SAR* results was studied. In order to understand the differences in *SAR* (or later in the temperature increase) between the skin, fat, and muscle tissues, not only the knowledge of in-depth wave propagation, but also the understanding about the properties of tissues from RF point of view is required, too. It can be concluded based on these simulations that when the antenna is used in the vicinity of high permittivity ε_r (e.g., $\varepsilon_{r\_SKIN} \approx 38$ @ 3 GHz and $\varepsilon_{r\_MUSCLE} \approx 52$) and high loss tangent of $tan\delta$ ($tan\delta_{SKIN} \approx 0.28$ @ 3 GHz and $tan\delta_{MUSCLE} \approx 0.25$) tissues, *SAR* and temperatures will be significantly high in comparison with fat tissue ($\varepsilon_{r\_FAT} \approx 5$ @ 3 GHz and $tan\delta_{FAT} \approx 0.15$). This can be explained due to the characteristics of tissues: skin and muscle have notable high water content and it will lead to the high power losses in RF frequencies. When the frequency goes higher, the losses in

TABLE III. TEMPERATURE RISE WITH THE TIME AND *PEAK INPUT POWERS* IN CASE THE ANTENNA CONTACTS THE TISSUE MODEL. INITIAL TEMPERATURE OF 36 ºC IS USED. MODEL M1 INCLUDES SKIN (T = 2 MM), FAT (T = 3 MM), AND MUSCLES (T = 30 MM), M2 ONLY SKIN (T = 35 MM), M3 FAT, AND M4 MUSCLES

Tissue Model	***Peak Input Power*** [mW]	**Bow-Tie Dipole**							**Single Loop**						
		Time [sec]						***Stationary solution***	***Time*** [sec]						***Stationary solution***
		120	240	360	480	600	720		120	240	360	480	600	720	
		Temperature [ºC]							***Temperature*** [ºC]						
M1	0.5	36.0	36.0	36.0	36.0	36.0	36.0	36.0	36.0	36.0	36.0	36.0	36.0	36.0	36.0
	50	36.1	36.2	36.3	36.3	36.3	36.3	36.6	36.0	36.0	36.0	36.0	36.0	36.0	36.4
	250	36.7	37.1	37.3	37.4	37.5	37.6	38.8	36.2	36.4	36.5	36.6	36.7	36.7	38.4
M2	0.5	36.0	36.0	36.0	36.0	36.0	36.0	36.0	36.0	36.0	36.0	36.0	36.0	36.0	36.0
	50	36.1	36.2	36.3	36.3	36.3	36.3	36.7	36.1	36.1	36.1	36.1	36.2	36.2	36.7
	250	36.7	37.1	37.3	37.5	37.6	37.8	39.4	36.3	36.5	36.6	36.7	36.8	36.9	39.6
M3	0.5	36.0	36.0	36.0	36.0	36.0	36.0	36.0	36.0	36.0	36.0	36.0	36.0	36.0	36.0
	50	36.0	36.0	36.0	36.0	36.0	36.1	36.2	36.0	36.0	36.0	36.0	36.0	36.1	36.2
	250	36.1	36.1	36.2	36.2	36.2	36.2	37.1	36.1	36.1	36.2	36.2	36.2	36.2	37.2
M4	0.5	36.0	36.0	36.0	36.0	36.0	36.0	36.0	36.0	36.0	36.0	36.0	36.0	36.0	36.0
	50	36.1	36.2	36.3	36.3	36.3	36.3	36.4	36.0	36.1	36.1	36.1	36.1	36.1	36.4
	250	36.7	37.1	37.3	37.4	37.5	37.6	38.2	36.2	36.3	36.4	36.5	36.5	36.6	38.0

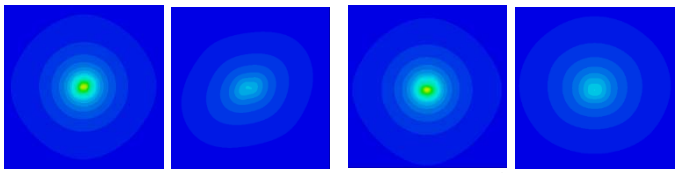

a) b)

Figure 3. Temperature distribution in *xy*-plane for a) dipole and b) loop antenna with different tissue models, when *PIP* of 50 mW is fed to the antenna: M1 (left), and M2 (right). Temperatures are scaled such that 36.0 ºC corresponds to blue, while red for 37.0 ºC. In each plot, cutting plane is aligned immediately below the antenna, at the top of tissue model.

high-permittivity tissues increase significantly.

2) Temperature

According to the lowest considered *PIP* of 0.5 mW, any temperatures over the initial temperature 36 ºC was not observed, even though different models were involved. By using notable higher powers of 50 mW or 250 mW, temperature rise in tissues was attained. Temperatures in Table III received by TSS correspond to the situations where temperature will not change anymore. Time-dependent solutions are shown in steps of 2 minutes.

Correspondingly with the *SAR*s, tissue characteristics are also observed to affect the obtained results with temperature. Fig. 3 further shows the temperature deviations of dipole and loop in *xy*-plane at the top of skin and fat models (for *PIP* of 50 mW). Temperature hot spot is the strongest right below the antenna and it decreases significantly with the distance away from the antenna. What comes to the differences between these tissue models, as explained in [1], the high thermal diffusivity of tissues is the reason why material reacts rapidly to the temperature of their surroundings. Therefore, due to high diffusivity, heat is conducted quickly in comparison to their volumetric heat capacity. That is one reason in order to explain the differences in the temperature rise and deviations in different tissues.

B. Comparing Investigated Antennas

As introduced at the beginning of Section III, exploited antennas were found to have FS performance very close to each other. One point we would like to mention is that the loop antenna configuration that authors have designed is found to have very similar radiation patterns with respect to the dipole, if comparison is made by positioning them next to each other, likewise in Fig. 1. That means that this UWB loop antenna generates its maxima of pattern in the direction of *z*-axis. The reason for this behaviour comes from the characteristics to operate like an electrically small antenna (ESA). If the antenna covers the entire FCC UWB band, it cannot be practically ESA at any rate in which case the patterns between dipole and loop according to the dual-theorem (dual patterns) can be achieved. Therefore, both the impedance behaviour and the patterns for the UWB loop differs from that what can be achieved with the typical electrically small single loop antenna.

Another interesting issue is that even though the UWB loop (or UWB dipole) do not behave like ESA in FS, however, in the proximity of body it acts like ESA, based on its impedance and radiation properties as concluded, e.g., in [14], [15]. Hence, authors would like to highlight that the presented antennas in this paper and their comparison is not like comparing typical dipole versus typical loop (because of the characteristics of ESA and the proximity of tissues).

Finally, during this study, noticeable differences between these two antennas however were not observed. *SAR* cross section cuttings below the antenna and also obtained temperature were relatively close to each other, and also other typical antenna parameters such as reflection coefficient S_{11} and total antenna efficiency behaved similarly. It could be remarked that even though corresponding temperatures in stationary situations will be achieved with these antennas, the temperature rise is slightly slower for loop.

IV. CONCLUSIONS AND FUTURE WORK

The effect of different peak input powers for different tissue models and two different UWB antennas were considered in this paper. The results of these evaluations is mainly to show how much power can be fed to the antenna in order the human

body tissues are immune to the harmful effects of EM radiation by an antenna (referring to the heating and *SAR*). Hence, this study experiments generally what should be the input power of the UWB antenna in order to cross the most commonly used *SAR* limits by IEEE and ICNIRP or in order the antenna start to heat the tissues. In pursuance of the evaluation of different input powers, these investigations also touched on the differences of antenna types. It was observed that tissues having high permittivity and loss tangent hence having notable high water content, e.g., skin and muscles, might cause more concern from *SAR* and temperature point of view than fat. These findings are further providing useful information for the most suitable position of implantable WBAN device.

As a possible future work, different body models (adult, child, female, and male) with the help of accurate voxel models of different cube resolutions will be involved to the studies, as used earlier for studies in lower frequencies [16].

Also, some additional parameters for more realistic simulation modelling will be included and taken into account such as the bloodflow coefficients (used to determine the influence of a blood at a certain temperature inside the tissue volume) and basal metabolic heat rate (an additional heating source taking the basal metabolic heat of biological tissue into account).

It would be also interesting to characterize whether the temperature and *SAR*s start to clearly diminish in some antenna orientations.

Further, *SAR* simulations are notably quite heavy and need a lot of memory in order to receive results in satisfactory and reasonable timing especially in high frequencies when the wavelength decreases and therefore required simulations mesh increases. Therefore, it is also of interest that would it be possible to significantly simplify *SAR* models for achieving realistic results, as the model simplification is proved to be productive [17].

One huge drawback in *SAR* investigations is the lack of measurement devices: they are expensive and not easily available, which causes uncertainty to verification of results.

V. ACKNOWLEDGEMENTS

This work is funded by the Finnish Funding Agency for Technology and Innovation (Tekes) through two research projects: Enabling future Wireless Healthcare Systems (EWiHS) and Wireless Body Area Network for Health and Medical Care (WiBAN-HAM). First author would like to acknowledge Tauno Tönning, Emil Aaltonen, TES and HPY foundations as well as to thank Ilari Hänninen from CST support for his multiple helpful advices with simulations.

REFERENCES

[1] D. A. Sânchez-Hernândez, High Frequency Electromagnetic Dosimetry. Norwood: Artech House, 2009, pp. 21-65.

[2] IEEE Recommended Practice for Measurements and Computations of Radio Frequency Electromagnetic Fields With Respect to Human Exposure to Such Fields, 100 kHz – 300 GHz, IEEE Std C95.3, 2002 (R2008).

[3] ICNIRP (International Commission on Non-Iodizing Radiation Protection), "Guidelines for limiting exposure to time-varying electric, magnetic, and electromagnetic fields (up to 300 GHz)," Health Phys., vol. 74, pp. 494-522, 1998.

[4] K. Chan, R. F. Cleveland, and D. L. Means, "Evaluating compliance with FCC guidelines for human exposure to radio frequency electromagnetic fields," FCC OET bulletin 65 (ed. 97-101) Supplement C, Washington, D.C., Dec. 1997.

[5] G. Kang, and O. P. Gandhi, "Effect of dielectric properties on the peak 1- and 10-g SAR for 802.11 a/b/g frequencies 2.45 and 5.15 to 5.85 GHz," IEEE Trans. Electrom. Comp., vol. 46, pp. 268-274, May 2004.

[6] Q. Wang, and J. Wang, "SA/SAR analysis for multiple UWB pulse exposure," in Proc. of Asia-Pacific Symp. & 19th Int. Zurich Symp. on Electromagn. Compat., May 2008, Singapore, pp. 212-215.

[7] M. Klemm, and G. Troester, "EM energy absorption in the human body tissues due to UWB antennas," Progress in Electromagn. Research, vol. 62, 2006, pp. 261-280.

[8] CST Microwave Studio [Online]. Available: http://www.cst.com.

[9] F.S. Barnes, and B. Greenebaum, Bioengineering and Biophysical Aspects of Electromagnetic Fields. Boca Raton: Taylor & Francis Group, 2007, pp. 58-59, 316-317 and 340-343.

[10] T. Tuovinen, M. Berg, K. Yekeh Yazdandoost, E. Salonen, and J. Iinatti, "Radiation properties of the planar UWB dipole antenna in the proximity of dispersive body models," in Proc. 7th Int. Conf. on BANs (BodyNets), Sep. 2012, Oslo, Norway, pp. 1-7.

[11] T. Tuovinen, M. Berg, K. Yekeh Yazdandoost, E. Salonen, and J. Iinatti, "Human body effect on the polarization properties of the new UWB dipole antenna in UWB WBAN applications," in Proc. 7th Int. Conf. on BANs (BodyNets), Sep. 2012, Oslo, Norway, pp. 1-7.

[12] T. Tuovinen, T. Kumpuniemi, K. Yekeh Yazdandoost, M. Hämäläinen, and J. Iinatti, "Effect of the antenna-human body distance on the antenna matching in UWB WBAN applications," 7th Int. Symp. Medical Inform. and Commun. Technol. (ISMICT 2013), March 2013, Japan, in press.

[13] Taconic (accessed on October 2012), TRF -41, -43, -45: Low-loss ceramic-filled PTFE [Online]. Available: http://www.taconic-add.com/pdf/trf.pdf.

[14] T. Tuovinen, M. Berg, K. Yekeh Yazdandoost, E. Salonen, and J. Iinatti, "Reactive near-field region radiation of planar UWB antennas close to a dispersive tissue model," in Proc. 8th Int. Loughborough. Ant. Propag. Conf. (LAPC), Nov. 2012, United Kingdom, pp. 1-4.

[15] T. Tuovinen, M. Berg, K. Yekeh Yazdandoost, E. Salonen, and J. Iinatti, "Impedance behaviour of planar UWB antennas in the vicinity of a dispersive tissue model," in Proc. 8th Int. Loughborough. Ant. Propag. Conf. (LAPC), Nov. 2012, United Kingdom, pp. 1-4.

[16] Q.-X. Li, and O. P. Gandfi, "Thermal implications of the new relaxed IEEE RF safety standard for head exposures to cellular telephones at 835 and 1900 MHz," IEEE Trans. Microw. Theory Tech., vol. 54, no. 7, pp. 3146-3154, July 2006.

[17] H. B. Lim, D. Baumann, and E.-P. Li, "A human body model for efficient numerical characterization of UWB signal propagation in wireless body area networks," IEEE Trans. Antennas Propag., vol. 58, no. 3, pp. 689-697, March 2011.